

Numerical Simulation of Breaking Waves on a Plane Slope with a Parallel Level Set Solver

M. Alagan Chella, H. Bihs & M. Muskulus

Department of Civil and Transport Engineering, Norwegian University of Science and Technology, Trondheim, Norway

ABSTRACT: In the present study, spilling breaking waves are simulated using a numerical model with interface capturing technique. The numerical model solves the Reynolds-Averaged Navier-Stokes (RANS) equations on a uniform Cartesian grid and complex geometry is modeled with a ghost cell immersed boundary method. The flow problem is solved as a two-phase flow of air and water with the free-surface is represented by the interface between the two phases. Thus, the level set method (LSM) is used to capture the complex free-surface changes. The temporal and spatial turbulent kinetic energy in the breaking waves is described by $k-\omega$ model. The conservative 5th order weighted essentially non-oscillatory (WENO) scheme is employed for the convective discretization. A much stronger coupling between velocity and pressure is obtained by using a staggered grid which is essential for a two phase model. The present model is fully parallelized using the message processing interface (MPI) library routines. The main focus of the present study is to investigate the wave breaking wave process over a sloping bed. The paper discusses the changes in the free surface profile, water surface envelope, and horizontal velocity in different regimes during the breaking process. Numerical experiments are carried out with the 5th order cnoidal waves on a plane slope 1/35. The present numerical model is validated and compared with the experimental data. The results from the numerical model are in good agreement with the experimental data concerning water surface envelope and horizontal velocity.

Keywords: Breaking waves, Wave breaking, CFD modelling, Free surface

1 INTRODUCTION

Breaking is initiated when the wave topography becomes steep then the wave becomes unstable and dissipates the energy in the form of turbulence, while a significant amount of air is trapped. Breaker types can be classified into four different types, namely spilling, plunging, surging and collapsing (Galvin, 1968). The breaking process is strongly influenced by the local water depth, wave steepness and sea bed slope. An exact numerical modeling of wave breaking process is intricate due to the strong non-linear air-sea interaction at the free surface, air entrainment and turbulent production, transport and dissipation process. Since there are many challenges to model the breaking process numerically, most of the studies on breaking waves are limited to field and experimental research. Ting and Kirby (1996) investigated the turbulent structures spilling breakers in the surf zone. Further, they studied the different wave breaking process between different types of breaking waves.

Longuet-Higgins and Cokelet (1976) first proposed a mixed Eulerian-Lagrangian formulation (MEL) based on potential theory to simulate breaking waves in deep water. Later, the method was modified the application to finite water depth by Vinje and Brevig (1981). However, most of the numerical models based on potential theory can describe the breaking process until breaking, but these model cannot model the impingement of the water jet during breaking (Chen et al., 1999). Wave breaking process can be described numerically with a model based on computational fluid dynamics (CFD) method without specifying breaking criteria. In addition to that most of the physical flow properties such as interface deformation, velocities and turbulence can be evaluated in detail. Numerous studies have attempted to simulate the breaking waves with a single phase viscous model which does not account the role of the air and the

density variation at the interface such as Bradford (2000); Lin and Liu (1998); Zhao et al. (2004). Further, it has been demonstrated that the importance of a two phase viscous flow models in the simulation of the breaking waves (Chen et al., 1999; Christensen, 2006; Hieu et al., 2004; Jacobsen et al., 2012). Moreover, these studies investigated turbulent characteristics and the undertow profiles. The present numerical model was utilized to study the wave transformation over a submerged reef with a slope of 1/10 with the 5th order Stokes waves and the main focus was to investigate the wave breaking process. The results from the numerical model showed a reasonable agreement with experimental data (Alagan Chella et al., 2013). The main focus of the present study is to investigate the breaking process with the changes in the free surface profile, wave surface elevation and the horizontal velocity. Moreover, the intention of the paper is to investigate the wave breaking process of spilling breakers over a sloping seabed using a two-phase flow three dimensional (3D) CFD model. The present 3D numerical model is utilized in a two dimensional (2D) setup to simulate the breaking waves over a sloping bed. To validate the present numerical model, the numerical results are compared with the experimental data by Ting and Kirby (1996). The changes in the free surface profile and velocity in different regimes are studied in the surf zone. The results from the numerical model are in good agreement with the experimental data concerning instantaneous free surface elevation, instantaneous horizontal velocity and wave group envelope.

2 NUMERICAL MODEL

2.1 Governing Equations

In the present study, the incompressible Reynolds-Averaged Navier-Stokes (RANS) equations are solved together with the continuity equation that describes the conservation of mass and the momentum. The governing equations are:

$$\frac{\partial U_i}{\partial x_i} = 0 \quad (1)$$

$$\frac{\partial U_i}{\partial t} + U_j \frac{\partial U_i}{\partial x_j} = -\frac{1}{\rho} \frac{\partial P}{\partial x_i} + \frac{\partial}{\partial x_j} \left[(v + \nu_t) \left(\frac{\partial U_i}{\partial x_j} + \frac{\partial U_j}{\partial x_i} \right) \right] + g_i \quad (2)$$

U is the velocity averaged over the time t , x is the spatial geometrical scale, ρ is the water density, ν is the kinematic viscosity, ν_t is the eddy viscosity, P is the pressure, and g is the gravitational constant. A staggered uniform Cartesian grid is used in the model in order to make the computational domain simple which enables the direct implementation of finite difference numerical schemes. Discretization of the convective term of the RANS equations is accomplished by the 5th order Weighted Essentially Non-Oscillatory (WENO) scheme (Jiang and Shu, 1996). This scheme has 3rd order accuracy for discontinuous solutions and has 5th order accuracy for a smooth solution. A 3rd order total variance diminishing (TVD) Runge-Kutta scheme, a three-step scheme is adopted for the time discretization (Shu and Osher, 1988).

The temporal and spatial turbulent kinetic energy in the breaking waves is described by the k - ω model (Wilcox, 1994). The two-equation model has two transport equations for the turbulent kinetic energy, k , and the specific turbulence dissipation, ω :

$$\frac{\partial k}{\partial t} + U_j \frac{\partial k}{\partial x_j} = \frac{\partial}{\partial x_j} \left[\left(\nu + \frac{\nu_t}{\sigma_k} \right) \frac{\partial k}{\partial x_j} \right] + P_k - \beta_k k \omega \quad (3)$$

$$\frac{\partial \omega}{\partial t} + U_j \frac{\partial \omega}{\partial x_j} = \frac{\partial}{\partial x_j} \left[\left(\nu + \frac{\nu_t}{\sigma_\omega} \right) \frac{\partial \omega}{\partial x_j} \right] + \frac{\omega}{k} \alpha P_k - \beta \omega^2 \quad (4)$$

where P_k is the production rate, and closure coefficients $\alpha = 5/9$, $\beta_k = 9/100$ and $\beta = 3/40$. A ghost cell immersed boundary method is implemented to describe the solid boundaries in the fluid domain and the algorithm is based on the local directional approach by Berthelsen and Faltinsen (2008). This methods avoids the explicit boundary conditions for the numerical discretization.

2.2 Free surface and wave generation

The description of the breaking process is demanding mainly due to the violent nonlinear free surface motion and a rapid transition of the wave shape. Hence, an accurate representation of the free surface is highly important to capture the interface deformation. The complex interface deformation is represented using the level set method (LSM) proposed by Osher and Sethian (1988). The free surface is described by the smooth signed level set function $\phi(\vec{x}, t)$ which is zero at the interface. In the computational cell, the sign of the function determines the phase of the fluid as follows:

$$\phi(\vec{x}, t) \begin{cases} > 0 & \text{if } \vec{x} \in \text{water} \\ = 0 & \text{if } \vec{x} \in \Gamma \\ < 0 & \text{if } \vec{x} \in \text{air} \end{cases} \quad (5)$$

The motion of the free surface is calculated using a convection equation for the level set function:

$$\frac{\partial \phi}{\partial t} + U_j \frac{\partial \phi}{\partial x_j} = 0 \quad (6)$$

The generation of waves at the inlet and absorption of waves at the outlet in the numerical wave tank is based on relaxation method concept. In this method, the computational wave is regulated by the analytical solution using a relaxation function in the relaxation zone and this has been presented by Mayer et al. (1998) and Engsig-Karup (2006). The relaxation function presented by Jacobsen et al. (2012) is employed in the present numerical model.

3 COMPUTATIONAL RESULTS AND DISCUSSION

3.1 Computational set-up and grid sensitivity study

In the numerical wave tank, a slope 1/35 is connected to a zone with constant water depth, $d=0.40\text{m}$ which resembles the laboratory setup by Ting and Kirby (1994) as shown in Figure 1. The wave kinematics in the wave generation region is obtained using the 5th order cnoidal wave theory proposed by Fenton (1999). The offshore wave height and the wave period at the constant water depth zone is $H_0=0.125\text{m}$ and $T=2.0\text{s}$ respectively. The free surface elevations and horizontal velocity are measured at different locations along the wave tank. The simulations are carried out for 25s of waves for the spilling breaker case.

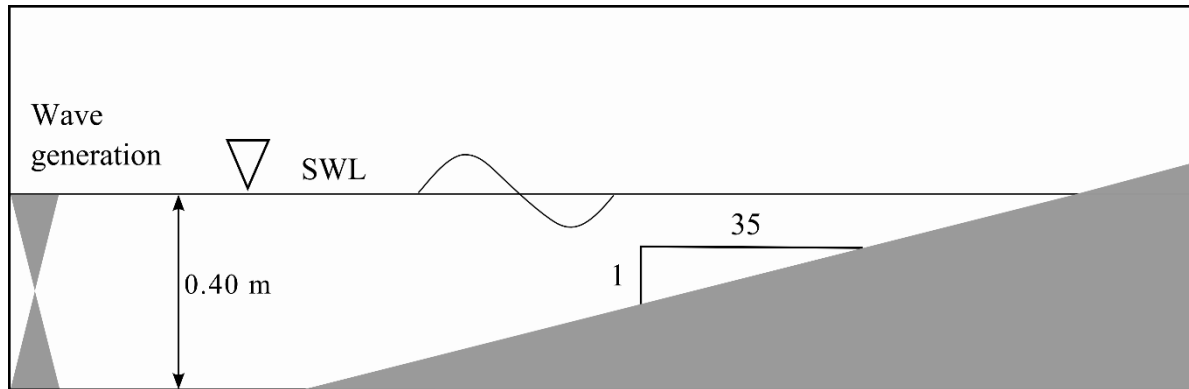


Figure 1. Computational domain

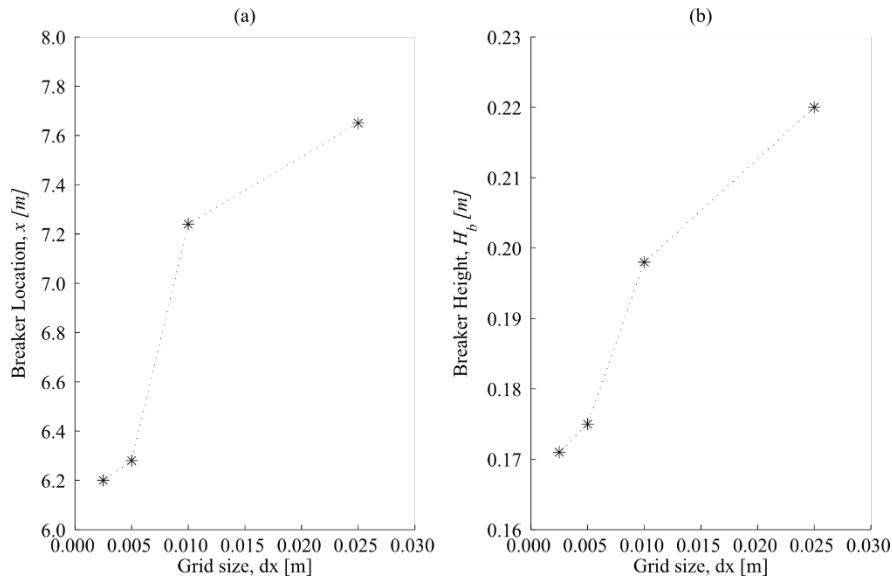


Figure 2. Grid sensitivity study on computed results (a) breaker location (x) and (b) breaker height (H_b)

The numerical model sensitivity to grid sizes is investigated with four different sizes $dx=0.025\text{m}$, 0.01m , 0.005m and 0.0025m . The influences of different grid sizes on the breaking point (x) and the breaker height (H_b) are considered and the simulated results are compared with the experimental data. Figure 2 shows the breaking point and the breaker height (H_b) versus the grid sizes. It appears that the breaking point and the breaker height decreases as the grid size decreases. The simulated waves on coarser grids ($dx=0.025\text{m}$ and $dx=0.01\text{m}$) break further offshore with higher breaker height. This might be due to the effect of lower numerical dissipation on coarser grids. However, the simulated waves on finer grids ($dx=0.005\text{m}$ and $dx=0.0025\text{m}$) yield good results. Finally, the simulated waves on grid size $dx=0.005\text{m}$ show good results with the experimental data ($x_b=6.4\text{m}$ and $H_b=0.165\text{m}$) with reasonable computational time.

3.2 Envelope of water surface elevation

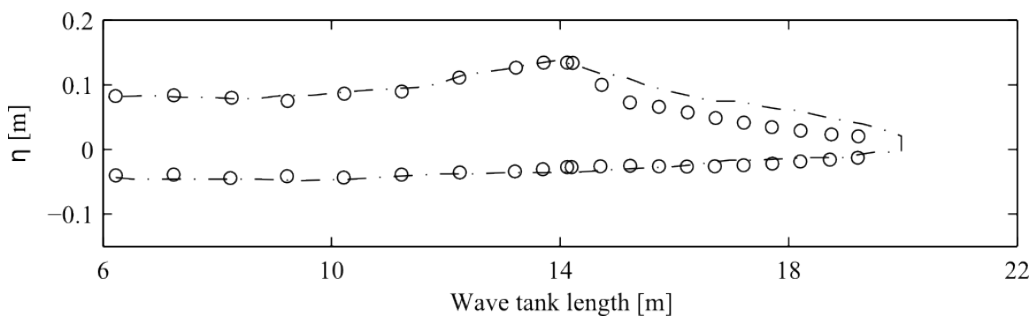


Figure 3. Comparison of simulated and measured envelope of water surface elevation. Dash-dot line: simulated results; circles: experimental data from Ting and Kirby (1996)

The computed results are compared with the experimental measurements for spilling breaker case by Ting and Kirby (1996). The comparison of computed and measured wave envelope is shown in Fig. 3. The wave height increases and the wave length decreases without the change in the wave period during shoaling. It appears that the wave crest becomes narrower and steeper with flatter trough as the wave propagates over the slope. In fact, the wave crest height increases continuously until reaches the breaking point and the wave height reduces after breaking. The simulated waves gradually steepen and break at $x_b=6.28\text{m}$ which is very close to the experimental breaking point at $x_b=6.4\text{m}$. Before and during breaking, the numerical results are in good agreement with the experimental data but the model slightly over predicts the wave crest after breaking. The reason could be the effects of the slower numerical dissipation of energy in the surf zone. On the whole, the simulated wave amplitudes are in good agreement with the experimental data.

3.3 Breaking wave kinematics in the surf zone

The horizontal velocity is measured over the depth with velocity probes at different locations in the surf zone shoreward along the tank. The surf zone can be divided into three sub zones namely, outer breaking zone, inner breaking zone and swash zone (Svendsen et al, 1978). The scope of the present study is limited to the wave transformation until the inner breaking zone. Figures 4, 5 and 6 show the changes in the horizontal velocity along the depth at three locations: in the outer breaker zone ($x=6.665\text{m}$), in the inner breaker zones ($x=7.725\text{m}$ and 7.885m). It appears that the horizontal velocity decreases as the wave propagates shoreward after breaking. In the roller region, the computed velocity in the wave trough as presented in the Figure 4 has some down spikes, but the velocity at the crest region matches very well with the experimental measurements. The wave profile at the breaking point is asymmetric. In the outer breaking zone, wave energy is transformed into turbulent kinetic energy including the formation of surface rollers with a rapid changes in the wave shape occurs (Peregrine and Svendsen, 2011).

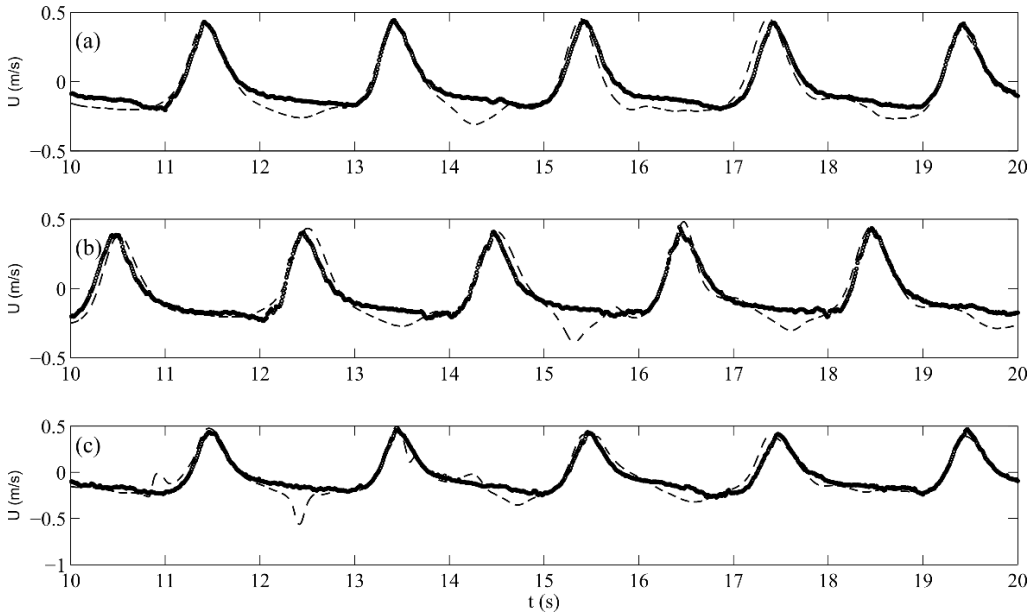


Figure 4. Comparison of simulated and measured horizontal velocity at $x=6.665\text{m}$ and $z=-0.17\text{m}$ (a), -0.15m (b), and -0.10m (c). Dashed lines: computed results; circles: experimental data from Ting and Kirby (1996)

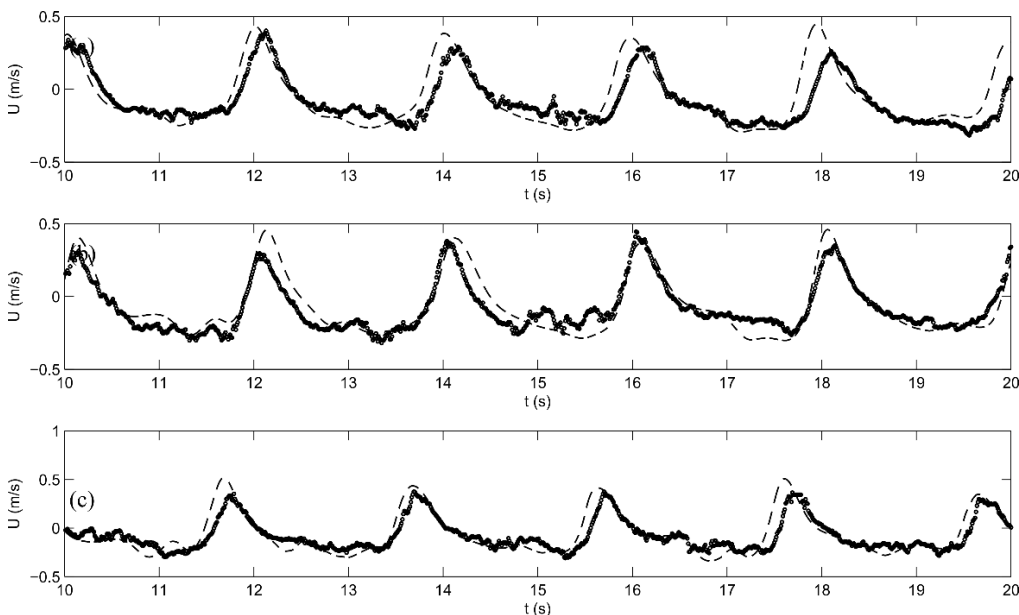


Figure 5. Comparison of simulated and measured horizontal velocity at $x=7.275\text{m}$ and $z=-0.14\text{m}$ (a), -0.10m (b) and -0.05m (c). Dashed lines: computed results; circles: experimental data Ting and Kirby (1996)

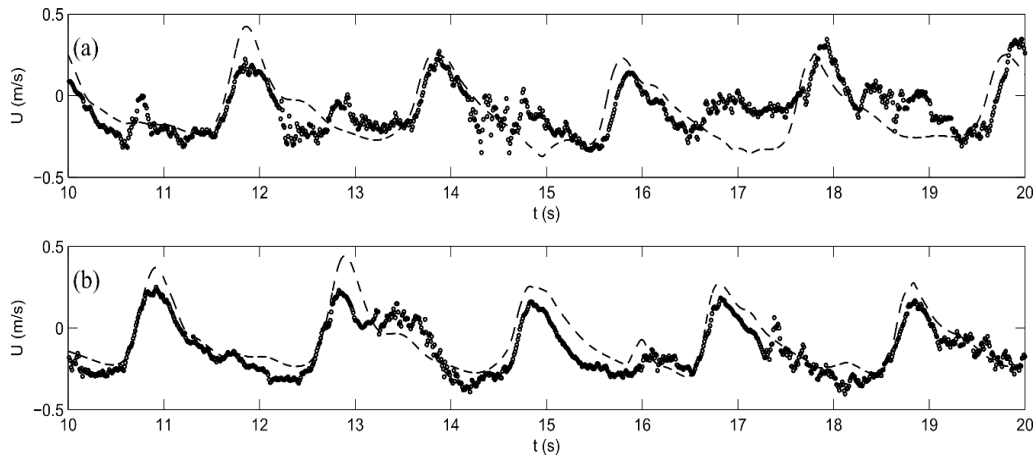


Figure 6. Comparison of simulated and measured horizontal velocity at $x=7.885$ m and $z=-0.10$ m (a) and -0.05 m (b). Dashed lines: computed results; circles: experimental data from Ting and Kirby (1996)

In fact, when the wave advances over the slope, it grows higher due to shoaling, giving rise to potential energy and accordingly, the wave crest particle velocities. Meanwhile, kinetic energy decreases slightly due to the reduction in the wave celerity, which is directly proportional to the water depth. As the wave grows further over the slope, the contribution of kinetic energy increases with increasing particle velocities in the high crest region. When the contribution of kinetic energy exceeds the contribution of potential energy to the total wave energy, a portion of the wave crest tends to move faster, resulting in a reduction of the wave height, which leads to a reduction in the potential energy. Hence, the reduction in the potential energy is converted into the kinetic energy of large vortices and roller motions. Further, the large vortices and roller motions are dissipated into the small scale surface turbulence in the inner breaking zone. The computed results clearly depicts that the horizontal velocity is maximum at the free surface and it decreases over depth. The difference between the computed and the measured horizontal velocity increases shoreward. It is noticed that the model slightly over predicts the wave amplitudes in the surf zone as shown in Figure 3. Although the reason for the over prediction is not fully known, this might be due to the slower dissipation of energy in the numerical model than in the experiments.

3.4 Wave profile and velocity variation during breaking process

Figure 7 shows the variation in the velocity and wave profile during the wave breaking process for spilling breakers. It appears that the velocity is higher near the vicinity of the wave crest and reaches the maximum value at the forward portion of the wave crest during breaking. The breaking process is strongly dominated by the local water depth and slope and moreover, these local physical parameters determine the characteristics of the breaking process i.e. energy dissipation and the shape of the wave. When waves approach the shoreline from deep to shallow water, the wave motion of the lower portion of the wave is strongly controlled by the change in water depth by seabed friction; e.g. the wave celerity is reduced. Therefore, the upper part of the wave propagates faster than the lower part and eventually breaking occurs. Since the particle velocity in the wave crest is larger than the wave celerity, the portion of the wave crest with larger particle velocity moves forward with a small scale water jet which resembles the development trend of plunging breaker. This is consistent with the previous studies (Lubin et al., 2011; Lader, 2002; Duncan, 2001). Furthermore the ejected wave front impinges the free surface which generates topological induced vorticity resulting in a pocket of air trapped inside the wave, the so-called splash-up phenomenon. Thus, the flow pattern is completely modified resulting in strong flow circulation.

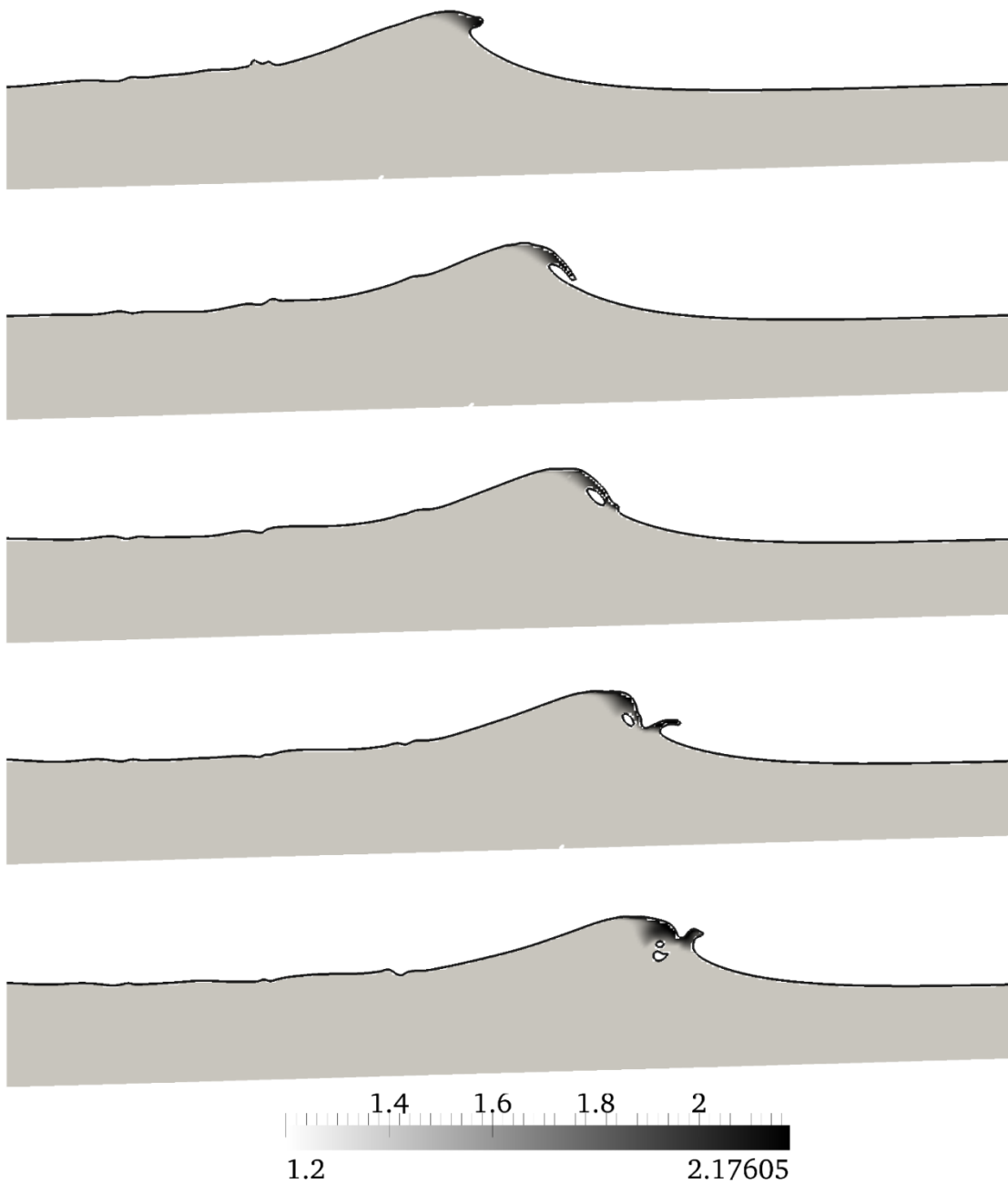


Figure 7. Velocity distribution and the free surface profile during the breaking process

4 CONCLUSIONS

A two-phase flow three dimensional CFD model based on RANS equations is used to investigate the breaking process over a sloping bed. The level set method and the $k-\omega$ turbulence model is used to describe the air-water interface and the free surface turbulence transport and dissipation during the breaking process respectively. The numerical results are compared with the experimental data by Ting and Kirby (1996) in terms of envelope of wave amplitudes and horizontal velocities for the spilling breaker case. The computed results are in good agreement with the experimental measurements. Moreover, the present model can describe the complete breaking process including the motion of air pockets in the water, formation of a forward moving jet, and the splash-up phenomenon. The results from the present study enhances the understanding of the prominent features associated with the wave breaking process over a sloping seabed.

ACKNOWLEDGEMENTS

The authors would like to thank Dr. James Kirby and Dr. Ting Francis for sharing the experimental data. The authors wish to acknowledge support from the Norwegian Research Center for Offshore Wind Technology (NOWITECH), Research council of Norway contract no.193823. The authors gratefully acknowledge the computing time granted by NOTUR (NN9240K) and provided on the Vilje system at the super computing facilities at NTNU.

REFERENCES

- Alagan Chella, M., Bihs, H., Kamath, A., Muskulus, M., (2013). Numerical modeling of breaking waves over a reef with a level set based numerical wave tank, Proceedings of 32nd International Conference on Offshore Mechanics and Arctic Engineering.
- Berthelsen, P.A., Faltinsen, O.M., (2008). A local directional ghost cell approach for incompressible viscous flow problems with irregular boundaries. *Journal of Computational Physics* 227, 4354–4397.
- Bradford, S.F., 2000. Numerical simulation of surf zone dynamics. *Journal of Waterway, Port, Coastal, and Ocean Engineering* 126, 1–13.
- Chen, G., Kharif, C., Zaleski, S., Li, J., (1999). Two-dimensional Navier–Stokes simulation of breaking waves. *Physics of Fluids* 11, 121–133.
- Christensen, E.D., (2006). Large eddy simulation of spilling and plunging breakers. *Coastal Engineering* 53, 463–485.
- Duncan, J.H., 2001. Spilling breakers. *Annual Review of Fluid Mechanics* 33, 519–547.
- Engsig-Karup, A.P., (2006). Unstructured Nodal DG-FEM Solution of High-order Boussinesq-type Equations. Ph.D. thesis. Technical University of Denmark.
- Fenton, J.D., (1999). The cnoidal theory of water waves. chapter 2. *Developments in Offshore Engineering*, Gulf, Houston, J. B. Herbich edition. pp. 55–100.
- Galvin, C.J., (1968). Breaker type classification on three laboratory beaches. *Journal of Geophysical Research* 73, 3651–3659.
- Hieu, P.D., Katsutoshi, T., Ca, V.T., (2004). Numerical simulation of breaking waves using a two-phase flow model. *Applied Mathematical Modelling* 28, 983–1005.
- Jacobsen, N.G., Fuhrman, D.R., Fredsøe, J., (2012). A wave generation toolbox for the open-source CFD library: OpenFoam. *International Journal for Numerical Methods in Fluids* 70, 1073–1088.
- Jiang, G.S., Shu, C.W., (1996). Efficient implementation of weighted ENO schemes. *Journal of Computational Physics* 126, 202–228.
- Lader, P.F., (2002). *Geometry and Kinematics of Breaking Waves*. Ph.D. thesis. Norwegian University of Science and Technology.
- Lin, P., Liu, P.L.F., (1998). A numerical study of breaking waves in the surf zone. *Journal of Fluid Mechanics* 359, 239–264.
- Longuet-Higgins, M.S., Cokelet, E.D., (1976). The deformation of steep surface waves on water I-A numerical method of computation, Proceedings of the Royal Society of London. Series A, Mathematical and Physical Sciences, pp. 1–26.
- Lubin, P., Glockner, S., Kimmoun, O., Branger, H., (2011). Numerical study of the hydrodynamics of regular waves breaking over a sloping beach. *European Journal of Mechanics - B/Fluids* 30, 552–564.
- Mayer, S., Garapon, A., Sørensen, L.S., (1998). A fractional step method for unsteady free surface flow with applications to nonlinear wave dynamics. *International Journal for Numerical Methods in Fluids* 28, 293–315.
- Osher, S., Sethian, J.A., (1988). Fronts Propagating with Curvature-Dependent Speed: Algorithms Based on Hamilton-Jacobi Formulations. *Journal of Computational Physics* 79, 12–49.
- Peregrine, D., Svendsen, I.A., (2011). Spilling breakers, bores and hydraulic jumps, Proceedings of the coastal engineering conference, pp. 540–550.
- Shu, C.W., Osher, S., (1988). Efficient implementation of essentially non-oscillatory shock capturing schemes. *Journal of Computational Physics* 77, 439–471.
- Svendsen, I.A., Madsen, P.A., Hansen, J.B., (1978). Wave Characteristics in the surf zone, Proceedings of the coastal engineering conference, pp. 520–539.
- Ting, F.C.K., Kirby, J.T., (1996). Dynamics of surf-zone turbulence in a spilling breaker. *Coastal Engineering* 27, 131–160.
- Vinje, T., Brevig, P., (1981). Numerical simulation of breaking waves. *Advances in Water Resources* 4, 77–82.
- Wilcox, D.C., (1994). *Turbulence Modeling for CFD*. DCW Industries Inc., La Canada, California.
- Zhao, Q., Armfield, S., Tanimoto, K., (2004). Numerical simulation of breaking waves by a multi-scale turbulence model. *Coastal Engineering* 51, 53–80.